

Thermal transport and quasi-normal modes in Gauss-Bonnet-axions theory

Xiao-Mei Kuang^{1*} and Jian-Pin Wu^{2,3†}

¹ *Instituto de Física, Pontificia Universidad Católica de Valparaíso, Casilla 4059, Valparaíso, Chile*

² *Institute of Gravitation and Cosmology, Department of Physics,*

School of Mathematics and Physics, Bohai University, Jinzhou 121013, China

³ *Shanghai Key Laboratory of High Temperature Superconductors, Shanghai, 200444, China*

Abstract

We obtain the black brane solution in arbitrary dimensional Gauss-Bonnet-axions (GBA) gravity theory. And then the thermal conductivity of the boundary theory dual to this neutral black brane is explored. We find that the momentum dissipation suppresses the DC thermal conductivity while it is enhanced by larger GB parameter. The analytical and numerical results of DC thermal conductivity match very well. Also we study the effect of the momentum dissipation and the GB coupling on the AC thermal conductivity and fit the results by Drude-like behavior for low frequency. Finally, we analytically compute the quasi-normal modes (QNM) frequency of the perturbative master field in large dimensions limit. Our analytical QNM frequencies agree well with the numerical results in large enough finite dimensions.

PACS numbers: 11.25.Tq, 04.50.Gh, 71.10.-w

*Electronic address: xmeikuang@gmail.com

†Electronic address: jianpinwu@mail.bnu.edu.cn

I. INTRODUCTION

The powerful holographic method, gauge/gravity duality[1–3], provides remarkable tools to explore diversity of strongly correlated systems in condensed matter physics through studying weakly coupled bulk gravitational theory[4–6]. More recently, to produce features of real materials, such as finite DC conductivity, we can introduce the momentum dissipation mechanism. There are several methods involved in to achieve the goal. One way is to introduce the so-called scalar lattice or ionic lattice, which is implemented by periodic scalar source or chemical potential[7–10]. Also, we can implement the momentum dissipation in the holographic massive gravity framework, which breaks the bulk diffeomorphism invariance and so that the momentum dissipates in the dual boundary field theory[11–16]. Another is holographic Q-lattice model in which the global phase of the complex scalar field breaks translational invariance[17–19]. Next but not the last is the models with massless scalar fields being linear dependent on the spatial directions, which is also named as linear axions [20–24].

In this paper, we shall construct the black brane solution in the framework of Gauss-Bonnet-axions (GBA). And then we numerically solve a gauge-invariant master field equation and obtain the thermal conductivity in five dimensional GBA theory. Also, we study the quasi-normal modes (QNM) spectrum by using the large spacetime dimension (large D) techniques.

The large D techniques, which is proposed in Ref.[25], is an efficient analytical tool to approximate finite D results of the equations in General Relativity as a perturbative calculation in expansion $1/D$. The main idea of the construction is that the large D limit localizes the gravitational field of the black hole in a near horizon region where the gravitational potential is very steep. This well-defined near horizon region splits the QNM spectrum into two different sets, decoupling modes and non-decoupling modes. The former modes squeezing only in the near horizon region, are normalizable states to all orders of $1/D$ and are sensitive to different black holes and capture specific properties. While the latter modes shared by many black holes can survive in the whole region and they are non-normalizable near horizon[26–28], so people are usually not interesting in the non-decoupled modes. The large D method has been applied to study the (in)stability of black holes[29–31]. In holographic framework, the large D method was used in [32] to pioneer to explore the analytical Drude behaviour beyond the hydrodynamic regime. The authors focused on the normalizable decoupling modes to analytically compute the QNM of the master field and AC thermal conductivity which agree well with the numerical results in the large D dimensional neutral black hole in Einstein-Axion theory.

The remaining of the paper is organized as follows. In section II, we solve the equations of motion derived from the GBA action and present the black brane solutions in $D = n + 3(n \geq 2)$ gravitational theory. Then we show the fluctuation equations of the neutral black hole in section III. In section IV, we study the thermal conductivity in GBA theory. Finally, in section V, we apply the large D method to analytically compute the QNM of the master perturbative field and compare the result with numerical one. The last section is our conclusion and discussion.

II. GAUSS-BONNET-AXIONS THEORY

We are interested in a specific thermal state, which holographically dual to the Gauss-Bonnet-axions (GBA) theory

$$S = \frac{1}{2\kappa^2} \int_d^{n+3} x \sqrt{-g} \left(R - 2\Lambda + \frac{\alpha}{2} \mathcal{L}_{GB} - \frac{1}{2} \sum_{I=1}^{n+1} (\partial\psi_I)^2 \right), \quad (1)$$

where ψ_I are a set of axionic fields, $2\kappa^2 = 16\pi G_{n+3}$ is the $n+3$ dimensional gravitational coupling constant and $\Lambda = -(n+1)(n+2)/2L^2$ is the cosmological constant. α is the GB coupling constant and

$$\mathcal{L}_{GB} = (R_{\mu\nu\rho\sigma} R^{\mu\nu\rho\sigma} - 4R_{\mu\nu} R^{\mu\nu} + R^2). \quad (2)$$

In what follows, we shall set $L = 1$.

With the action, the equations of motion are easily obtained as

$$\begin{aligned} \nabla_\mu \nabla^\mu \psi_I &= 0, \\ R_{\mu\nu} - \frac{1}{2} g_{\mu\nu} \left(R + (n+1)(n+2) + \frac{\alpha}{2} (R^2 - 4R_{\rho\sigma} R^{\rho\sigma} + R_{\lambda\rho\sigma\tau} R^{\lambda\rho\sigma\tau}) \right) \\ &+ \frac{\alpha}{2} (2RR_{\mu\nu} - 4R_{\mu\rho} R_\nu^\rho - 4R_{\mu\rho\nu\sigma} R^{\rho\sigma} + 2R_{\mu\rho\sigma\lambda} R_\nu^{\rho\sigma\lambda}) - \sum_{I=1}^{n+1} \left(\frac{1}{2} \partial_\mu \psi_I \partial_\nu \psi_I - \frac{g_{\mu\nu}}{4} (\partial\psi_I)^2 \right) = 0. \end{aligned} \quad (3)$$

We take the form of the scalar fields linearly depending on the $n+1$ spatial direction x^a as ¹

$$\psi_I = \beta \delta_{Ia} x^a, \quad (4)$$

which is responsible for the momentum dissipation in the dual field theory. And then, a homogeneous and isotropic neutral black brane solution is admitted

$$ds^2 = -f(r) dt^2 + \frac{1}{f(r)} dr^2 + \frac{r^2}{L_e^2} dx^a dx^a, \quad (5)$$

where, after defining $\hat{\alpha} = n(n-1)\alpha/2$,

$$f(r) = \frac{r^2}{2\hat{\alpha}} \left(1 - \sqrt{1 - 4\hat{\alpha} \left(1 - \frac{r_h^{n+2}}{r^{n+2}} \right) + \frac{2\hat{\alpha} L_e^2 \beta^2}{r^2 n} \left(1 - \frac{r_h^n}{r^n} \right)} \right). \quad (6)$$

Here r_h satisfying $f(r_h) = 0$ is the black brane horizon. The GB coupling parameter $\hat{\alpha}$ is constrained by no negative energy fluxes condition and causality of the dual CFT into the range[33]²

$$- \frac{n(3n+8)}{4(n+4)^2} \leq \hat{\alpha} \leq \frac{n(n-1)(n^2+3n+8)}{4(n^2+n+4)^2}. \quad (7)$$

Then, via the standard method, the Hawking temperature of the black brane is

$$T = \frac{f'(r_h)}{4\pi} = \frac{1}{4\pi} \left((n+2)r_h - \frac{L_e^2 \beta^2}{2r_h} \right). \quad (8)$$

¹ In general, the linear combination form of the scalar fields are $\psi_I = \beta_{Ia} x^a$. Then defining a constant $\beta^2 \equiv \frac{1}{n+1} (\sum_{a=1}^{n+1} \sum_{I=1}^{n+1} \beta_{Ia} \beta_{Ia})$ with the coefficients satisfying the condition $\sum_{I=1}^{n+1} \beta_{Ia} \beta_{Ib} = \beta^2 \delta_{ab}$, we will get the same black hole solution. Since there is rotational symmetry on the x^a space, we can choose $\beta_{Ia} = \beta \delta_{Ia}$ without loss of generality.

² Note that this result is given in the case without the axionic fields. Additional constraints may be required due to the introduction of axionic fields and we shall address this problem in future. In this paper, we will take the constraint (7).

And the entropy density of horizon is

$$s = \frac{r_h^{n+1}}{4G_{n+3}}. \quad (9)$$

Near the UV boundary $r \rightarrow \infty$,

$$f(r) \sim \frac{1 - \sqrt{1 - 4\hat{\alpha}}}{2\hat{\alpha}} r^2. \quad (10)$$

So the effective asymptotic AdS radius is

$$L_e^2 = \frac{2\hat{\alpha}}{1 - \sqrt{1 - 4\hat{\alpha}}} \rightarrow \begin{cases} 1, & \text{for } \hat{\alpha} \rightarrow 0 \\ \frac{1}{2}, & \text{for } \hat{\alpha} \rightarrow \frac{1}{4} \end{cases}. \quad (11)$$

The Einstein limit is obtained by taking $\hat{\alpha} \rightarrow 0$, in which the gravitational background recovers the solution addressed in [20]. In addition, it is worth to point out that at zero temperature, the near horizon geometry is $AdS_2 \times \mathbb{R}^{n+1}$ with the AdS_2 radius $L_2 = \frac{1}{n+2}$. Note that to have a unit velocity of light, the metric component g_{ii} in Eqs. (5) and (6) are dependent of GB coupling parameter $\hat{\alpha}$. They are somewhat different from one presented in [22] where $g_{ii} = r^2/L^2$ is independent of GB coupling $\hat{\alpha}$. This requirement shall result in different conclusion as we see later.

III. LINEARIZED PERTURBATIVE EQUATIONS

To study the heat transport, we turn on the following consistent linearized perturbation about the background (5) as

$$\delta g_{tx} = e^{-i\omega t} r^2 h_{tx}(r), \quad \delta \psi_1 = e^{-i\omega t} S(r)/\beta. \quad (12)$$

And then the equations of motion can be evaluated as

$$i\omega \left(2\hat{\alpha} - \frac{r^2}{f} \right) h'_{tx} + S' = 0, \quad (13)$$

$$S'' + \left(\frac{n+1}{r} + \frac{f'}{f} \right) S' + \frac{\omega^2}{f^2} S - \frac{i\omega L_e^2 \beta^2}{f^2} h_{tx} = 0, \quad (14)$$

which govern the dynamics of the perturbations. The prime in equations above denotes the derivative to the radius coordinate r . Near the boundary $r \rightarrow \infty$, the behavior of these fields is

$$h_{tx} = h_{tx}^{(0)} + \frac{h_{tx}^{(n+2)}}{r^{n+2}} + \dots, \quad (15)$$

$$S = S^{(0)} + \frac{(\omega^2 S^{(0)} - i\omega \beta^2 h_{tx}^{(0)})/2n}{r^2} + \dots. \quad (16)$$

Note that for even n , the above behaviors should have extra logarithms terms due to the Weyl anomaly appearing in the even boundary dimensions. To solve the equations of motion (13) and (14), the purely ingoing conditions for the perturbations shall be imposed near the horizon as

$$h_{tx} \sim h_1 (r - r_h)^{-i\omega/4\pi T}, \quad (17)$$

$$S \sim S_1 (r - r_h)^{-i\omega/4\pi T}. \quad (18)$$

It is convenient to package the linearized equations (13) and (14) into a gauge invariant master field equation

$$\Phi'' + \left(\frac{f'}{f} + \frac{n-1}{r} \right) \Phi' + \left(\frac{\omega^2}{f^2} + \left(\frac{nf'}{rf} - \frac{2n}{r^2} \right) - \frac{L_e^2 \beta^2}{f(r^2 - 2\hat{\alpha}f)} \right) \Phi = 0, \quad (19)$$

where

$$\Phi(r) = \frac{rf(r)S'(r)}{i\omega}. \quad (20)$$

Near the horizon, the master equation satisfies the ingoing conditions

$$\Phi \sim (r - r_h)^{-i\omega/4\pi T} \quad (21)$$

where we set the regular coefficient to be unit. Near the boundary, we have

$$\Phi = \begin{cases} \Phi^{(0)} + \frac{\Phi^{(n)}}{r^n} + \dots, & \text{for } n = \text{odd} \\ \Phi^{(0)} + \frac{\Phi^{(n)}}{r^n} + \frac{L_e^{2n} \omega^n \Phi^{(0)}}{Nr^n} \log r + \dots, & \text{for } n = \text{even} \end{cases} \quad (22)$$

where the dots denote the higher order terms and N depends on the dimension n . Thus, $\Phi^{(0)}$ and $\Phi^{(n)}$ can be treated as the source and thermal current function of the master field Φ , respectively. And the Green function which is related with the thermal conductivity $\kappa(\omega)$ is

$$\kappa(\omega) = \frac{iG(\omega)}{\omega T} = \begin{cases} \frac{1}{i\omega T} \frac{n\Phi^{(n)}}{L_e^{n+1}\Phi^{(0)}}, & \text{for } n = \text{odd} \\ \frac{1}{i\omega T} \left(\frac{n\Phi^{(n)}}{L_e^{n+1}\Phi^{(0)}} - \frac{L_e^{n-1}\omega^n}{N} \right), & \text{for } n = \text{even} \end{cases}, \quad (23)$$

Compared with the asymptotic behaviors of fields h_{tx} and S ((15) and (16)) and (20), we have

$$\Phi^{(0)} = \frac{i\omega S^{(0)} + \beta h_{tx}^{(0)}}{n}, \quad \Phi^{(n)} = \frac{(n+2)\beta^2}{\omega^2} h_{tx}^{(n+2)}. \quad (24)$$

And then the thermal conductivity can also read off from the boundary behavior of the perturbation h_{tx} and S .

Before proceeding, to simplify our problems, we shall redefine the bulk parameters as

$$\tilde{\alpha} = n\hat{\alpha}, \quad \tilde{\beta} = \frac{\beta}{\sqrt{n}}. \quad (25)$$

Furthermore, in the calculation of thermal conductivity, we shall use $\hat{\beta} \equiv \tilde{\beta}/T$, which is the only one scaling-invariant quantity of the black brane (5) with (6) for a given GB parameter. Also we set $r_h = 1$ in numerical calculation.

IV. THERMAL CONDUCTIVITY

A. DC thermal conductivity

In this subsection, we study the DC thermal conductivity. Following the method outlined in [22, 34], we analytically derive the dimensionless DC thermal conductivity as

$$\kappa_0/T = \frac{(4\pi)^2 r_h^{n+1}}{nL_e^2 \tilde{\beta}^2}. \quad (26)$$

Now we set $r_h = 1$ and summarize its features as follows.

- Form Eq. (26), it is easily observed that when $\tilde{\beta}$ goes to zero, κ_0 is divergent, which originates from the translational invariance and the momentum is conserved. When the momentum dissipates, i.e., $\tilde{\beta}$ is finite, κ_0/T becomes finite. In particular, for fixed geometry parameters n and $\tilde{\alpha}$, κ_0/T decreases as $\tilde{\beta}$ increases.
- FIG. 1 exhibits κ_0/T as a function of the GB parameter $\tilde{\alpha}$ for fixed $\tilde{\beta}$ and n . It indicates that the DC thermal conductivity is enhanced by positive GB gravity while is suppressed by negative GB coupling. It is worthwhile to note that, our observation is different from that shown in [22] where the κ_0 is independent of the GB coupling. The reason is the same as we have emphasized that to have unite speed of light, our metric component should be $g_{ii} = r^2/L_e^2$, which depend on $\tilde{\alpha}$.
- κ_0/T decreases with the increase of the spacetime dimensions.

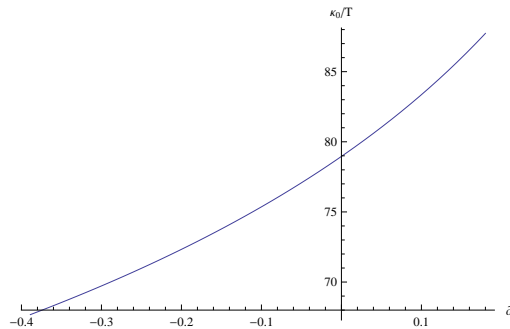


FIG. 1: DC thermal conductivity κ_0 as a function of the GB parameter $\tilde{\alpha}$ with fixed $n = 2$ and $\tilde{\beta} = 1$.

Next we turn to the study of AC thermal conductivity.

B. AC thermal conductivity

In this subsection, we study the AC thermal conductivity in five dimensional GBA gravity theory, i.e., $n = 2$, in which $\tilde{\alpha}$ is $-7/18 \leq \tilde{\alpha} \leq 9/50$. FIG.2 shows the dissipation effect ($\hat{\beta}$) on the thermal conductivity in GBA gravity theory, while FIG.3 exhibits the GB coupling effect on the thermal conductivity for small momentum dissipation (left plot in FIG.3) and large momentum dissipation (right plot in FIG.3) respectively.

Firstly, as a quick check on the consistency of our numerics, we denotes the DC thermal conductivity analytically calculated by Eq. (26) (red dots) in FIG.2 and FIG.3. They match very well with the numerical results.

And then, we focus on the momentum dissipation effect. Since the momentum dissipates, we have finite DC thermal conductivity in GBA gravity theory as one in Schwarzschild-axions (SA) theory [32, 35]. For small momentum dissipation, the AC thermal conductivity exhibits a Drude-like peak at low frequency. With the increase of $\hat{\beta}$, the peak gradually becomes a valley, which indicates a crossover from coherent to incoherent phase. Quantitatively, for small $\hat{\beta}$, we can fit the low frequency AC thermal conductivity in terms of the Drude-like formula (right plot in FIG.2),

$$\kappa(\omega) = \frac{K\tau}{1 - i\omega\tau} \quad (27)$$

where K is a constant and τ is the relaxation time. The corresponding fitting results of K and τ with $n = 2$ and $\tilde{\alpha} = 9/50$ are listed in TABLE I.

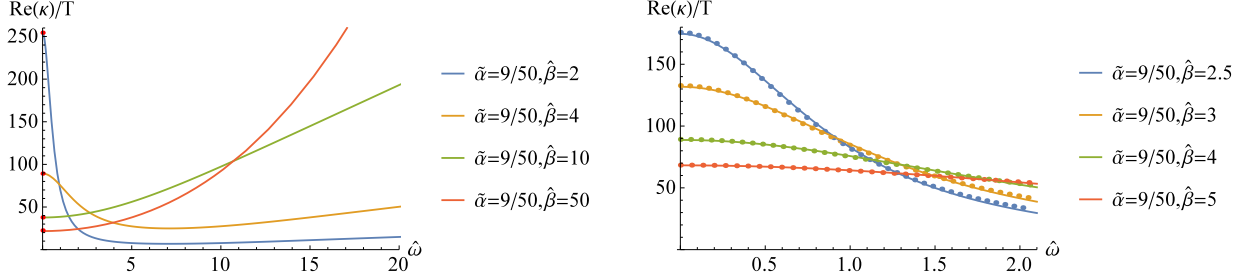


FIG. 2: AC thermal conductivity $\kappa(\omega)$ with fixed $\tilde{\alpha} = 9/50$ for different $\hat{\beta}$. The red dots at zero frequency in left plot are the analytic DC values calculated by (26). Right plot: The dots are the numerical results while the solid lines are fitted by (27).

$\hat{\beta}$	2	2.5	3	4	5
K	155.296	165.737	178.74	213.90	271.15
τ	1.630	1.053	0.737	0.414	0.251

TABLE I: Fitting parameters for different $\hat{\beta}$ with fixed $n = 2$ and $\tilde{\alpha} = 9/50$.

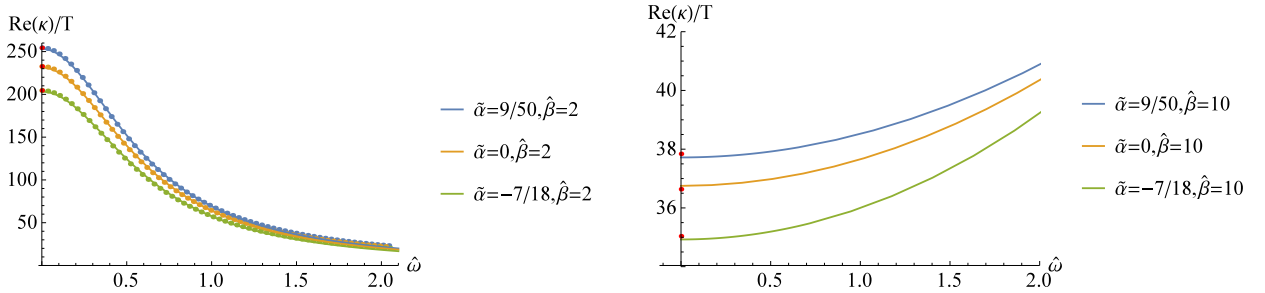


FIG. 3: AC thermal conductivity $\kappa(\omega)$ with different $\tilde{\alpha}$ for fixed $\hat{\beta}$. Left plot is for $\hat{\beta} = 2$, in which the dots are the numerical results while the solid lines are fitted by (27). Right plot is for $\hat{\beta} = 10$.

Moreover, we explore the effect of GB parameter on the AC thermal conductivity (FIG.3). For small $\hat{\beta}$, the peak at low frequency conductivity decreases with the decrease of GB coupling parameter $\tilde{\alpha}$ and the relaxation time τ decrease (TABLE II). While for large $\hat{\beta}$, with the decrease of the GB coupling, the valley in low frequency conductivity becomes deeper. Nonetheless, for fixed $\hat{\beta}$ we cannot have a crossover from coherent to incoherent phase (or vice versa) by only changing $\tilde{\alpha}$ in the allowed region of $\tilde{\alpha}$.

V. QUASI-NORMAL MODES

We turn to study the QNM spectrum of the master field of the perturbation by the so-called Large n method, which is proposed and extensively studied in [26–28]. The Large n technique provides an analytical method to perturbatively solve the above master equation by treating $1/n$ as a small parameter. As it is addressed in [26–28], the spectrum of QNM in the large n limit can be split into decoupled modes and non-decoupled modes, of which the former are always normalisable in the near horizon geometry and unique

$\tilde{\alpha}$	9/50	0	-7/18
K	155.28	143.28	127.76
τ	1.629	1.614	1.589

TABLE II: Fitting parameters for different $\tilde{\alpha}$ with fixed $n = 2$ and $\hat{\beta} = 2$.

for different black hole, while the latter are not normalisable and have common features for many black holes. In [32], the authors claimed that the decoupled modes indeed controlled the ‘Drude poles’ of the conductivity in the boundary theory dual to the Einstein-Maxwell-axion gravity. In this subsection, we will use the Large n method to analytically calculate the decoupled QNM for the master field Φ and then compare them with the numerical results.

To this end, we rewrite the master equation (19) with the tortoise coordinate $dr_* = \frac{dr}{f(r)}$

$$\left(\frac{d^2}{dr_*^2} + \omega^2 - V \right) \Psi = 0, \quad (28)$$

where we rescale $\Phi = r^{\frac{1-n}{2}} \Psi$ and the potential is

$$V = \frac{(n+1)f(2rf' - (n+3)f)(r^2 - 2\hat{\alpha}f) - 4L_e^2\beta^2 r^2 f}{4r^2(r^2 - 2\hat{\alpha}f)}. \quad (29)$$

To guarantee the existence of the decoupled QNM, the effective potential should have a negative minima [26–28]. FIG. 4 shows the profile of the potential for some parameters. We see it presents a negative minima, which means that there exists the decoupled QNM of the master field.

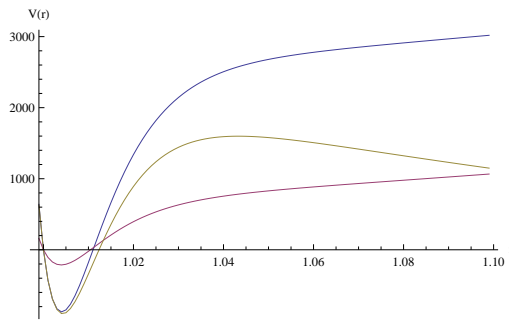


FIG. 4: The effective potential for different samples of bulk parameters.

To calculate the QNM of the decoupled mode in large n limit, we introduce

$$\rho = (r/r_h)^n. \quad (30)$$

and expand the master field and the frequency as

$$\Phi = \sum_{k \geq 0} \frac{\Phi_k}{n^k}, \quad \omega = \sum_{k \geq 0} \frac{\omega_k}{n^k}. \quad (31)$$

Then, putting (30) and (31) into the master equation (19), and expand it in the power of the small quantity $1/n$, we can obtain series equation of motion for Φ_k .

Before solving the equations for each order Φ_k , we have to fix their boundary conditions. In order to get the behavior of each order Φ_k near the horizon, we insert the expansion (31) into the condition (21), then

solve behavior at each order

$$\begin{aligned}
\Phi_0(\rho \rightarrow 1) &\rightarrow 1, \\
\Phi_1(\rho \rightarrow 1) &\rightarrow -\frac{2i \log(\rho - 1)\omega_0}{2 - L_e^2 \tilde{\beta}^2}, \\
\Phi_2(\rho \rightarrow 1) &\rightarrow \frac{2i \log(\rho - 1)(4\omega_0 + i \log(\rho - 1)\omega_0^2 - (2 - L_e^2 \tilde{\beta}^2)\omega_1)}{(2 - L_e^2 \tilde{\beta}^2)^2}, \\
&\dots\dots\dots
\end{aligned} \tag{32}$$

Near AdS boundary, the decoupled mode is normalisable, so that we have the behavior

$$\Phi_k(\rho \rightarrow \infty) \rightarrow 0. \tag{33}$$

Integrating the series equation of motion order by order and considering the boundary conditions (32) and

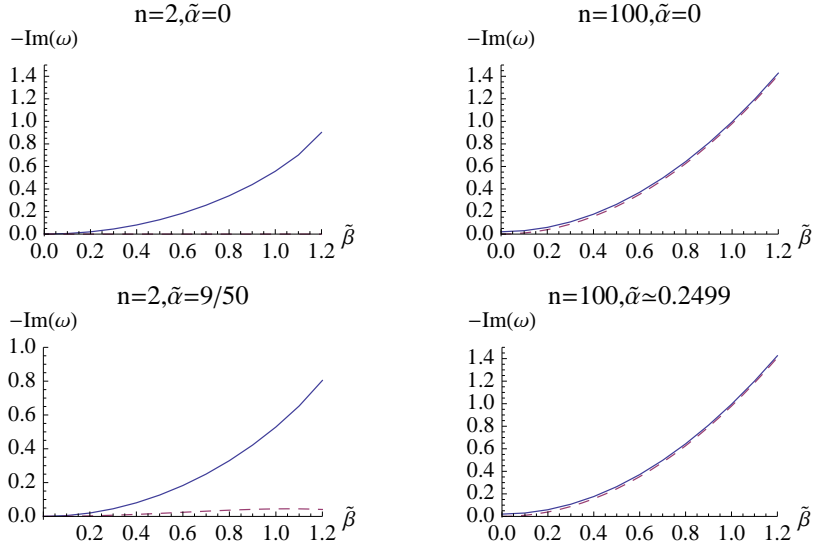


FIG. 5: Imaginary part of QNM frequency as a function of $\tilde{\beta}$ with fixed GB coupling $\tilde{\alpha} = n\hat{\alpha}$. In each plot, solid line are numerical result, while the dashed line denotes analytical result drawn via the formular (35).

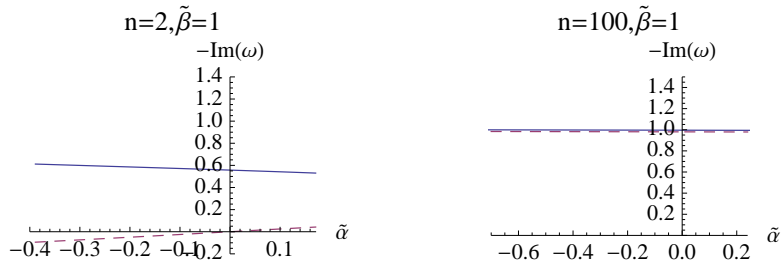


FIG. 6: Imaginary part of QNM frequency as a function of the GB coupling $\tilde{\alpha} = n\hat{\alpha}$ with fixed axion $\tilde{\beta}$. Solid lines are numerical results, while the dashed lines are analytical results drawn via the formular (35).

(33), we can get the exact solution of Φ_0 , Φ_1 and Φ_2 and the frequency to the first order

$$\begin{aligned}
\omega_0 &= -iL_e^2 \tilde{\beta}^2, \\
\omega_1 &= 2iL_e^2 \tilde{\beta}^2 - \frac{i\tilde{\alpha}L_e^2 \tilde{\beta}^2 (2 - L_e^2 \tilde{\beta}^2)}{2}.
\end{aligned} \tag{34}$$

So that to the order n^{-1} , the decoupled QNM frequency for Φ is

$$\omega = -iL_e^2\tilde{\beta}^2 \left(1 + \frac{1}{n} \frac{\tilde{\alpha}(2 - L_e^2\tilde{\beta}^2) - 4}{2} + O(n^{-2}) \right). \quad (35)$$

Note that in the Einstein limit $\tilde{\alpha} = 0$, this result recovers that shown in [32]. Due to the complex of our metric, we can only obtain the solution of Φ_k up to the second order. Correspondingly the frequency mode we can obtained here is up to the order of n^{-1} .

We move on to compare our analytical QNM frequency (35) with the numerical results. In FIG. 5, we fix the scaled GB coupling $\tilde{\alpha}$ and study the effect of the scaled Axion momentum $\tilde{\beta}$ on the imaginary part of QNM frequency. We choose a small $n = 2$ black brane for the left panel, while in the right panel, we have $n = 100$. We see that the analytical results (dashed) agree well with the numerical results (solid) for large enough finite n shown in the plots of the right panel. FIG. 6 shows the imaginary part of QNM frequency as a function of the scaled GB coupling $\tilde{\alpha} = n\hat{\alpha}$ with fixed non-vanishing axion. It is also obvious that the analytical and numerical results are almost consistent for large enough dimension in the right plot.

VI. CONCLUSION AND DISCUSSION

In this paper, we construct a new neutral black brane solution from the GBA gravity theory in any dimensional AdS spacetimes. The thermal conductivity of the dual theory of this black brane geometry is explored. For small momentum dissipation, the optical conductivity exhibits a Drude-like peak at low frequency region. With the increase of the momentum dissipation, a transition from coherent to incoherent phase happens as has been revealed in (SA) theory [32, 35]. However, we can not observe an apparent transition from coherent to incoherent phase when we tune the GB coupling parameter only in the allowed region but fix the momentum dissipation parameter.

Also, via the large dimension technique, we analytically study the QNM of the master field which control heat transport of the dual system. The analytical frequency of QNM agrees well with the numerical one when the dimension is large enough. However, we would like to point out that here we only obtain the solution of mast field up to the second order as well as the frequency mode up to the order of n^{-1} and we can not observe the breakdown of the perturbative expansion, which can be seen as a signature of the coherent/incoherent transition as pointed out in [32]. It would be very interesting to improve the computation skill to solve higher order equation of the master field so that we can test the robustness observed in [32].

In addition, we can also study the electric and heat transport by adding a gauge field term $S_M = \frac{1}{2\kappa^2} \int d^{n+3}x \sqrt{-g} \left(-\frac{1}{4} F_{\mu\nu} F^{\mu\nu} \right)$ into the action (1). An analytical charged black brane solution can be obtained as following

$$A_t(r) = \mu \left(1 - \frac{r_h^n}{r^n} \right), \quad (36)$$

$$f(r) = \frac{r^2}{2\hat{\alpha}} \left(1 - \sqrt{1 - 4\hat{\alpha} \left(1 - \frac{r_h^{n+2}}{r^{n+2}} \right) + \frac{2\hat{\alpha}}{r^2} \left(\frac{n\mu^2 r_h^n}{(n+1)r^n} + \frac{L_e^2\beta^2}{n} \right) \left(1 - \frac{r_h^n}{r^n} \right)} \right), \quad (37)$$

where μ is understood as the chemical potential of the dual field theory on the boundary. The properties of transport of this charged black brane geometry and it related QNM shall be addressed somewhere else.

Acknowledgments

We are grateful to Kentaro Tanabe for helpful correspondence. We also thank Yi Ling, Wei-Jia Li and Xiang-Rong Zheng for valuable discussions. X. M. Kuang is supported by Chilean FONDECYT grant No.3150006. J. P. Wu is supported by the Natural Science Foundation of China under Grant Nos.11305018 and 11275208, by Natural Science Foundation of Liaoning Province under Grant Nos.201602013, and by the grant (No.14DZ2260700) from the Opening Project of Shanghai Key Laboratory of High Temperature Superconductors.

-
- [1] J. M. Maldacena, “The large N limit of superconformal field theories and supergravity,” *Adv. Theor. Math. Phys.* **2** (1998) 231 [*Int. J. Theor. Phys.* **38** (1999) 1113].
 - [2] S. S. Gubser, I. R. Klebanov and A. M. Polyakov, “A semiclassical limit of the gauge string correspondence,” *Nucl. Phys. B* **636** (2002) 99.
 - [3] E. Witten, “Anti-de Sitter space and holography,” *Adv. Theor. Math. Phys.* **2** (1998) 253.
 - [4] S. A. Hartnoll, “Lectures on holographic methods for condensed matter physics,” *Class. Quant. Grav.* **26**, 224002 (2009) [arXiv:0903.3246 [hep-th]].
 - [5] C. P. Herzog, “Lectures on Holographic Superfluidity and Superconductivity,” *J. Phys. A* **42**, 343001 (2009) [arXiv:0904.1975 [hep-th]].
 - [6] N. Iqbal, H. Liu and M. Mezei, “Lectures on holographic non-Fermi liquids and quantum phase transitions,” arXiv:1110.3814 [hep-th].
 - [7] G. T. Horowitz, J. E. Santos and D. Tong, “Optical Conductivity with Holographic Lattices,” *JHEP* **1207**, 168 (2012) [arXiv:1204.0519 [hep-th]].
 - [8] G. T. Horowitz, J. E. Santos and D. Tong, “Further Evidence for Lattice-Induced Scaling,” *JHEP* **1211**, 102 (2012) [arXiv:1209.1098 [hep-th]].
 - [9] A. Donos and S. A. Hartnoll, “Interaction-driven localization in holography,” *Nature Phys.* **9**, 649 (2013) [arXiv:1212.2998 [hep-th]].
 - [10] Y. Ling, C. Niu, J. P. Wu and Z. Y. Xian, “Holographic Lattice in Einstein-Maxwell-Dilaton Gravity,” *JHEP* **1311**, 006 (2013) [arXiv:1309.4580 [hep-th]].
 - [11] D. Vegh, “Holography without translational symmetry,” arXiv:1301.0537 [hep-th].
 - [12] R. A. Davison, “Momentum relaxation in holographic massive gravity,” *Phys. Rev. D* **88**, 086003 (2013) [arXiv:1306.5792 [hep-th]].
 - [13] M. Blake and D. Tong, “Universal Resistivity from Holographic Massive Gravity,” *Phys. Rev. D* **88**, no. 10, 106004 (2013) [arXiv:1308.4970 [hep-th]].
 - [14] M. Blake, D. Tong and D. Vegh, “Holographic Lattices Give the Graviton an Effective Mass,” *Phys. Rev. Lett.* **112**, no. 7, 071602 (2014) [arXiv:1310.3832 [hep-th]].
 - [15] A. Amoretti, A. Braggio, N. Maggiore, N. Magnoli and D. Musso, “Analytic dc thermoelectric conductivities in holography with massive gravitons,” *Phys. Rev. D* **91**, no. 2, 025002 (2015) [arXiv:1407.0306 [hep-th]].
 - [16] Z. Zhou, J. P. Wu and Y. Ling, “DC and Hall conductivity in holographic massive Einstein-Maxwell-Dilaton gravity,” *JHEP* **1508**, 067 (2015) [arXiv:1504.00535 [hep-th]].
 - [17] A. Donos and J. P. Gauntlett, “Holographic Q-lattices,” *JHEP* **1404**, 040 (2014) [arXiv:1311.3292 [hep-th]].
 - [18] A. Donos and J. P. Gauntlett, “Novel metals and insulators from holography,” *JHEP* **1406**, 007 (2014) [arXiv:1401.5077 [hep-th]].
 - [19] Y. Ling, P. Liu and J. P. Wu, “A novel insulator by holographic Q-lattices,” *JHEP* **1602**, 075 (2016) [arXiv:1510.05456 [hep-th]].
 - [20] T. Andrade and B. Withers, “A simple holographic model of momentum relaxation,” *JHEP* **1405**, 101 (2014) [arXiv:1311.5157 [hep-th]].
 - [21] K. Y. Kim, K. K. Kim, Y. Seo and S. J. Sin, “Coherent/incoherent metal transition in a holographic model,” *JHEP* **1412**, 170 (2014) [arXiv:1409.8346 [hep-th]].
 - [22] L. Cheng, X. H. Ge and Z. Y. Sun, “Thermoelectric DC conductivities with momentum dissipation from higher derivative gravity,” *JHEP* **1504**, 135 (2015) [arXiv:1411.5452 [hep-th]].
 - [23] X. H. Ge, Y. Ling, C. Niu and S. J. Sin, “Thermoelectric conductivities, shear viscosity, and stability in an anisotropic linear axion model,” *Phys. Rev. D* **92**, no. 10, 106005 (2015) [arXiv:1412.8346 [hep-th]].
 - [24] T. Andrade, “A simple model of momentum relaxation in Lifshitz holography,” arXiv:1602.00556 [hep-th].
 - [25] R. Emparan, R. Suzuki and K. Tanabe, “The large D limit of General Relativity,” *JHEP* **1306**, 009 (2013) [arXiv:1302.6382 [hep-th]].
 - [26] R. Emparan and K. Tanabe, “Universal quasinormal modes of large D black holes,” *Phys. Rev. D* **89**, no. 6, 064028 (2014) [arXiv:1401.1957 [hep-th]].

- [27] R. Emparan, R. Suzuki and K. Tanabe, “Decoupling and non-decoupling dynamics of large D black holes,” JHEP **1407**, 113 (2014) [arXiv:1406.1258 [hep-th]].
- [28] R. Emparan, R. Suzuki and K. Tanabe, “Quasinormal modes of (Anti-)de Sitter black holes in the $1/D$ expansion,” JHEP **1504**, 085 (2015) [arXiv:1502.02820 [hep-th]].
- [29] R. Emparan, R. Suzuki and K. Tanabe, “Instability of rotating black holes: large D analysis,” JHEP **1406**, 106 (2014) [arXiv:1402.6215 [hep-th]].
- [30] K. Tanabe, “Instability of the de Sitter Reissner-Nordstrom black hole in the $1/D$ expansion,” Class. Quant. Grav. **33**, no. 12, 125016 (2016) [arXiv:1511.06059 [hep-th]].
- [31] B. Chen and P. C. Li, “Instability of Charged Gauss-Bonnet Black Hole in de Sitter Spacetime at Large D ,” arXiv:1607.04713 [hep-th].
- [32] T. Andrade, S. A. Gentle and B. Withers, “Drude in D major,” JHEP **1606**, 134 (2016) [arXiv:1512.06263 [hep-th]].
- [33] A. Buchel, J. Escobedo, R. C. Myers, M. F. Paulos, A. Sinha and M. Smolkin, “Holographic GB gravity in arbitrary dimensions,” JHEP **1003**, 111 (2010) [arXiv:0911.4257 [hep-th]].
- [34] A. Donos and J. P. Gauntlett, “Thermoelectric DC conductivities from black hole horizons,” JHEP **1411**, 081 (2014) [arXiv:1406.4742 [hep-th]].
- [35] R. A. Davison and B. Goutraux, “Momentum dissipation and effective theories of coherent and incoherent transport,” JHEP **1501**, 039 (2015) [arXiv:1411.1062 [hep-th]].